ELSEVIER

Polymer 42 (2001) 7017–7023

polymer

www.elsevier.nl/locate/polymer

Changes in structural and mechanical behaviour of PVDF with processing or thermal treatment. 2. Evolution of mechanical behaviour

Badr-Eddine El Mohajir*, Nicole Heymans

Université Libre de Bruxelles, Physique des Matériaux de Synthèse. CP 194/08, 84 av. A. Buyl, 1050 Brussels, Belgium

Received 19 October 1999; received in revised form 28 February 2001; accepted 2 March 2001

Abstract

The following study is the continuation of our previous work, which consisted in analysing the structural evolution of PVDF after different thermomechanical treatments. In this second part, we will discuss the influence of these evolutions on the mechanical behaviour. This has been determined by tensile drawing, creep or dynamic measurements.The observed changes in behaviour are strongly influenced by the different processing routes. Therefore, the beta conformation appears only when stretching injection-moulded samples (IM) and is accompanied by an increase of rupture stress compared to yield stress, which is not the case for compressed samples (CM). The influence of annealing on mechanical behaviour varies with annealing and measurement temperature. Thus, annealing at 80°C after standardisation increases the Young's modulus at 120°C and decreases it during drawing at 23°C compared to other annealing treatments.

Keywords: PVDF; Thermomechanical history; Tensile drawing

1. Introduction

The mechanical behaviour of a polymer is closely linked to its amorphous and crystalline phases and their interfacial region. The main factor that controls its properties is the chain conformation in the solid state, which depends strongly on the crystallisation and therefore on the thermomechanical history of the polymer [1]. In the case of PVDF [2], slow cooling will allow the spherolites nucleated in the first stages of cooling to grow rather than interacting with other crystalline zones. This reduces the interfacial region and increases the degree of order of the system, so Young's modulus and yield stress are higher than after quenching. After the latter, there are more crystals but of small size, and therefore the interfacial region is increased.

Several authors have studied the molecular mechanisms that appear during the deformation of semi-crystalline polymers [3–7]. The complexity of these deformation mechanisms is strongly related to the crystalline phase, which may be deformed by a range of mechanisms, such as slipping, twinning, or martensitic transformations. These are the mechanisms proposed by Peterlin [3]. Molecular mechanisms studied during PVDF drawing indicates that necking resembles melting-recrystallisation, the mechanism of plastic deformation of a semi-crystalline polymer proposed by Flory and Yoon [8].

Study of mechanical relaxation of PVDF indicates three main relaxations [9]: γ relaxation (around -80°C) is attributed to local chain movement; β relaxation, or lower glass transition, (around -32°C) is attributed to a large amplitude motion of the main chain; and, finally, α relaxation, or upper glass transition, (around 40°C) is attributed to motion of molecular chains in folds at the lamellae surfaces [10,11].

We have discussed in the previous paper [12], the effects of different thermomechanical treatments on PVDF structure. In this paper, we will discuss the influence of these treatments and therefore of structural evolution on its mechanical behaviour, with drawing, dynamic and creep measurements.

2. Experimental

A full description of all materials used and their treatments are given in the first part of this work [12].

PVDF samples, of type ISO 1B, were prepared by injection moulding (IM) or cut from compression moulded plates (CM).

* Corresponding author. Tel.: +32-2-650-2759; fax: +32-2-650-2766.
E-mail address: bmohajir@ulb.ac.be (B.-E. El Mohajir).

0032-3861/01/$ - see front matter
PII: S0032-3861(01)00184-7

2.1. Tensile drawing measurements:

Samples were drawn in an Instron tensile tester. Two displacement rates were chosen, 0.1 and 0.01 cm/min, which correspond to deformation rates of $16e^{-3}$ and $16e^{-4}$ s^{-1} respectively. Measurements were taken at three temperatures: 23, 40 and 120°C. Young's modulus, yield and fracture stress and strain were obtained from these measurements.

2.2. Creep measurements:

Creep measurements were taken at 23 and 40°C for IM samples. The creep stress depends on temperature; the stress values were chosen in relation to the yield stress as determined by the tensile drawing measurements. Thus we have chosen the values of 70, 80 and 90% of yield stress at a displacement rate of 0.1 cm/min. Measurements were taken by an extensometer connected to a data acquisition system.

2.3. Dynamic measurements:

The experimental procedure is given in the first part of this work [12].

3. Experimental results

3.1. Effects of processing technique

Phenomena appearing during tensile drawing depend strongly on the nature of the sample (injected or pressed) and measurement temperature. For IM, deformation is homogeneous at 23 or 40°C (Fig. 1), which is not the case for CM; thus we observe localised deformation and the appearance of necking which propagates along the sample

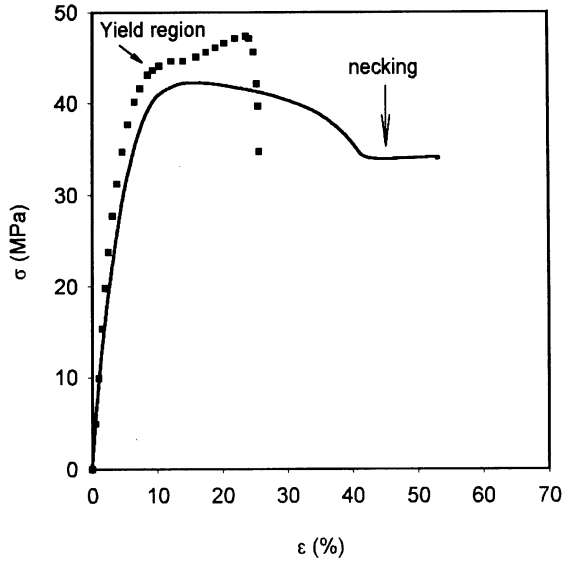

Fig. 1. Tensile drawing curves at 23°C for IM (square) and CM (full line) as-delivered samples; displacement rate = 0.01 cm/min.

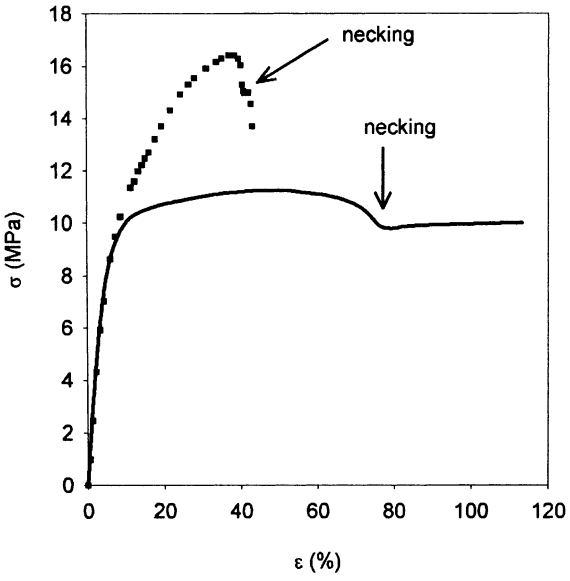

Fig. 2. Tensile drawing curves at 120°C for IM (A: square) and CM (B: full line) as-delivered samples; displacement rate = 0.01 cm/min.

and is accompanied by material whitening. Note that during tensile drawing at 120°C (Fig. 2), necking also appears for IM.

Tensile drawing measurement uncertainty is 1% in stress. We obtain two kinds of curves as shown in Fig. 1. Major differences appear after yield, thus we observe a stress increase for IM (squares), whereas maximum stress is reached at yield for CM (full line). Also IM reaches rupture just after stress is maximised, while CM reaches a higher fracture strain after necking. This necking appears also in IM but only when drawn at 120°C (Fig. 2) and remains lower compared to CM where maximal stress is reached just before necking and not at yield.

To compare the effects of treatments on the tensile drawing curves, we define several quantities in order to illustrate the differences. For example, for IM linear deformation, we took as reference the stress value for 10% strain and the strain value for 30 MPa stress, respectively σ_{I10} and ϵ_{I30} (Fig. 1).

In IMB (Injection moulded samples containing β conformation), necking is also observed (Fig. 3), even when drawing at 23 or 40°C and rupture occurs at a higher deformation than in IM.

On increasing the deformation rate, no qualitative changes are observed but differences between samples are enhanced. Other characteristic values were taken as the maximum stress reached and the corresponding strain, $\sigma_{I,Cmax}$ and $\epsilon_{I,Cmax}$, respectively, also the drawing stress for CM, σ_{Cd} which corresponds also to the stress before rupture at ϵ_{Cr}.

Tables 1–5 summarize the characteristic values of the tensile drawing curves IM and CM. The slope at the origin, corresponding to the Young's modulus, is the only feature independent of the sample nature.

According to the tables, we note that the Young's modulus

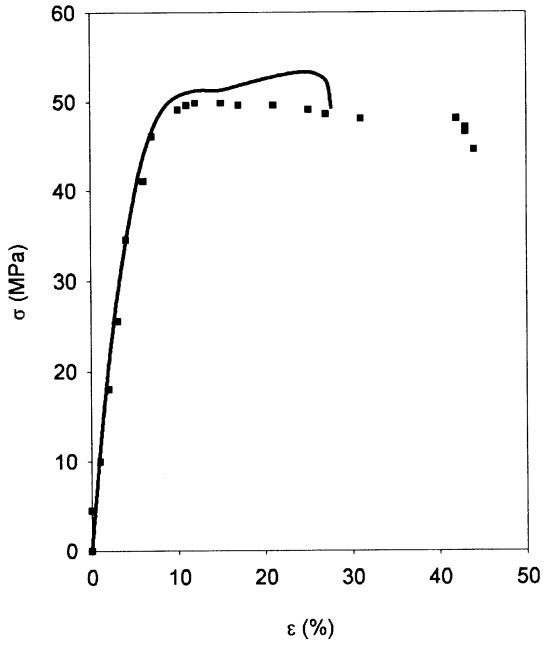

Fig. 3. Tensile drawing curves at 23°C for IM (full line) and IMB (square) samples annealed for 10 days at 80°C; displacement rate = 0.01 cm/min.

is slightly higher for pressed samples, as is the storage modulus. This is more obvious at 40 and 120°C. But IM samples reach a higher stress than CM ones. The maximum stress for IM is reached before rupture on drawing at 23 or 40°C, and before necking, which precedes rupture when drawing at 120°C. For CM, necking before rupture occurs even when drawing at 23 or 40°C. In these latter cases, maximum stress is reached in the yield range, while during drawing at 120°C, it is reached just before necking.

In both cases, for IM and CM samples, deformation at maximum stress increases with temperature.

Concerning extension, CM are more extensible than IM, thus rupture deformation exceeds 120% during the drawing of CM at 120°C and only reaches 50% for IM.

3.2. Effects of standardisation annealing:

The aim of this treatment is to erase the sample's thermo-

Table 1
All stresses and deformations are nominal, displacement rate = 0.01 cm/min. I: Injected sample IM; E: Young's modulus; ϵ_{I30}: deformation for σ equal to 30 MPa; σ_{I10}: stress for ϵ equal to 10%; drawing at 23°C

Treatment	E_I MPa	ϵ_{I30} %	σ_{I10} MPa	σ_{Imax} MPa	ϵ_{Imax} %
As-delivered	1041	3.5	44	47.36	23.66
Standardised	918	4.6	43	48.85	24
+1 day 23°C	962	4.6	42	47.61	24.5
+10 days 23°C	1030	4	44	48.55	24.3
+1 day 40°C	1031	4	45	49.34	22.8
+10 days 40°C	1065	4	45	48.46	24.16
+1 day 80°C	931	4.4	44	48.35	24.16
+10 days 80°C	886	4.4	44	49.88	25.66

Table 2
All stresses and deformations are nominal, displacement rate = 0.01 cm/min. I: Injected sample IM; E: Young's modulus; ϵ_{I30}: deformation for σ equal to 30 MPa; σ_{I10}: stress for ϵ equal to 10%; drawing at 40°C

Treatment	E_{IM} MPa	ϵ_{I30} %	σ_{I10} MPa	σ_{Imax} MPa	ϵ_{Imax} %
As-delivered	769	6.3	35	40.46	23.83
Standardised	703	6.6	35	40.3	24.25
+1 day 23°C	749	6.5	35	40.79	24.16
+10 days 23°C	769	6.4	35.5	40.55	25.5
+1 day 40°C	783	6	36.5	40.83	25.83
+10 days 40°C	782	5.8	36	40.79	25.08
+1 day 80°C	731	6.3	35.5	40.22	26
+10 days 80°C	756	5.8	35.8	40.51	23

mechanical history. Indeed when comparing two types of samples, one having undergone annealing during 30 days at 40°C and the other not, we notice that even if their behaviour in drawing is different before standardisation, it becomes identical afterwards (Fig. 4).

We will now compare the behaviour of the as-delivered samples and those that have undergone a standardisation annealing. This behaviour depends on sample type (IM or CM) and measurement temperature. For tests carried out at 23 and 40°C, the modifications are almost identical (Fig. 4, Tables 1–4). Thus, we notice a decrease of Young's

Table 3
All stresses and deformations are nominal, displacement rate = 0.01 cm/min. C: Compressed sample CM; E: Young's modulus; σ_{Cmax}: maximum stress; ϵ_{Cmax}: deformation corresponding to σ_{Cmax}, in case of IM, ϵ_{Imax} = rupture deformation; σ_{Cn}: necking stress; ϵ_{Cr}: rupture deformation; drawing at 23°C

Treatment	E_C MPa	σ_{Cmax} MPa	ϵ_{Cmax} %	σ_{Cn} MPa	ϵ_{Cr} %
As-delivered	1046	42.43	11.16	32.74	59.83
Standardised	914	42.25	14.66	34.1	54.33
+1 day 23°C	1028	42.71	14	34.6	60.3
+10 days 23°C	1186	45.46	12	35.58	42.3
+1 day 40°C	1148	44.72	11.83		
+10 days 40°C	1161	46.43	11.66	35.82	57.33
+1 day 80°C	1012	43.76	13.66	35.17	43
+10 days 80°C	1094	45.31	13.16	35.74	45.16

Table 4
All stresses and deformations are nominal, displacement rate = 0.01 cm/min. C: Compressed sample CM; E: Young's modulus; σ_{Cmax}: maximum stress; ϵ_{Cmax}: deformation corresponding to σ_{Cmax}, in case of IM, ϵ_{Imax} = rupture deformation; σ_{Cn}: necking stress; ϵ_{Cr}: rupture deformation; drawing at 23°C

Treatment	E_C MPa	σ_{Cmax} MPa	ϵ_{Cmax} %	σ_{Cn} MPa	ϵ_{Cr} %
As-delivered	918	37.34	13.16	28.48	> 60
Standardised	815	35.41	14	28.57	> 45
+1 day 23°C	904	36.78	14.16	29.09	> 50
+10 days 23°C	956	37.82	14	30.33	> 45
+1 day 40°C	1012	37.43	12.16	30.23	> 50
+10 days 40°C	1040	38.09	12.16	30.60	68.16
+1 day 80°C	803	37.07	13.83	29.86	> 45
+10 days 80°C	918	38.13	13.5	30.34	65.16

Table 5
All stresses and deformations are nominal, displacement rate = 0.01 cm/min. C: Compressed sample CM, E: Young's modulus; σ_{Cmax}: maximum stress; ϵ_{Cmax}: deformation corresponding to σ_{Cmax}, in case of IM, ϵ_{Imax} = rupture deformation; σ_{Cn}: necking stress; ϵ_{Cr}: rupture deformation; drawing at 120°C

Treatment	E_C MPa	σ_{Cmax} MPa	ϵ_{Cmax} %	σ_{Cn} MPa	ϵ_{Cr} %
As-delivered	220	11.23	44	10	> 120
Standardised	280	11.06	37.66	10.09	> 120
+1 day 23°C	263	10.96	42.83	10.06	> 120
+10 days 23°C	257	11.22	38.5	10.28	> 120
+1 day 40°C	230	11.09	44	10.2	> 120
+10 days 40°C	264	11.08	41.83	10.06	> 120
+1 day 80°C	303	11.02	40.16	9.81	> 120
+10 days 80°C	331	10.98	37.33	10.05	> 120
	E_{IM} MPa	σ_{Imax} MPa	ϵ_{Imax} %	σ_{In} MPa	ϵ_{Ir} %
+10 days 80°C	230	16.61	28.33	14.9	38

modulus after standardisation, for IM as well as for CM samples. Similarly, the yield stress decreases and the yield strain increases whilst the stress before rupture increases, leading to curves crossing. This trend is confirmed by creep measurements (Fig. 5) when measuring the compliance, which increases after standardisation at short times, and decreases at long times and high deformations, also leading to curves crossing.

When testing at 120°C, the observed changes are different (Fig. 6, Table 5). We note rather an increase of Young's modulus after standardisation, as well as an increase of yield stress and decrease of yield strain.

This is in agreement with measurements of the dynamic storage modulus, which decreases in the region of the upper glass transition (the case of 23 and 40°C measurement temperature) and increases at high temperatures (the case of 120°C).

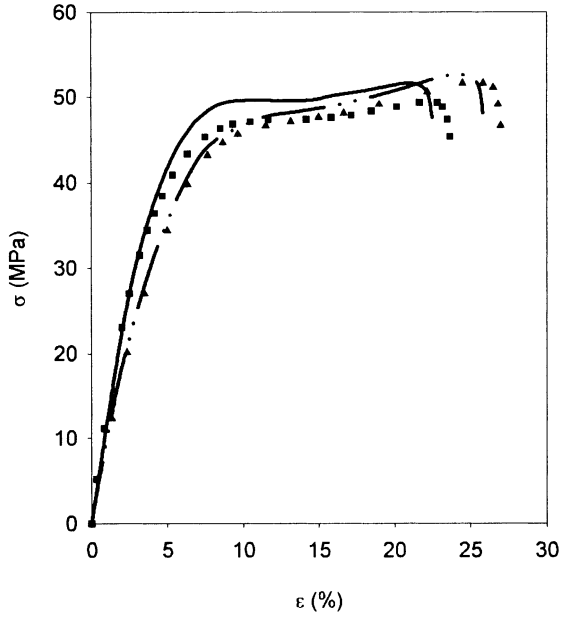

Fig. 4. Tensile drawing curves at 23°C for IM samples as-delivered (square) and standardised (dash-dot-dot), annealed 30 days at 40°C (full line) and standardised (triangle); displacement rate = 0.01 cm/min.

3.3. Effects of post-standardisation annealing

DMA measurements [12] show that these treatments do not affect the storage modulus at low or high temperatures, but only at room temperature, just below the upper glass transition. We note an increase of storage modulus after annealing at 23 and 40°C compared with that after standardisation or at 80°C both for IM and CM.

In drawing and creep measurements, annealing effects are apparent as from the early stages of deformation. These vary with measurement temperature.

The influence of annealing time depends on temperature. This is more visible for IM in tensile tests at 23°C. Thus when annealing at 40 or 80°C, saturation is reached after 1 day, so ϵ_{I30} and σ_{I10} are equal to those after 10 days annealing. This not the case following annealing at 23°C. Furthermore we observe that the tensile curve obtained after 1 day annealing at 40°C is very close to that after 10 days at 23°C (Fig. 7).

E_N, E_{23}, E_{40} and E_{80} will be used to denote Young's modulus after standardisation, 23, 40 and 80°C annealing, respectively.

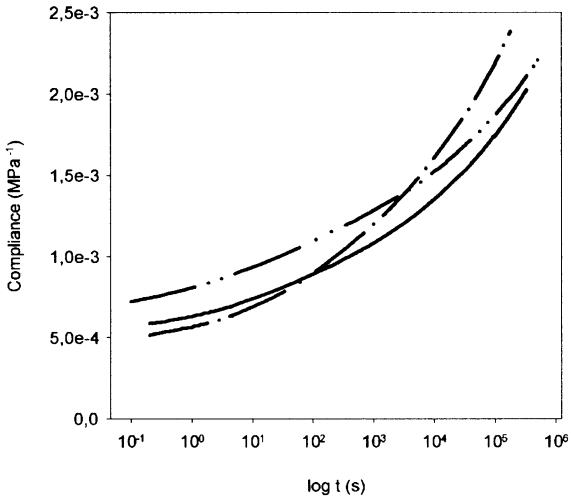

Fig. 5. Creep curves at 23°C of IM sample as-delivered (dash-dot), standardised (dash-dot-dot) and annealed 10 days at 40°C (full line); applied stress = 32 MPa.

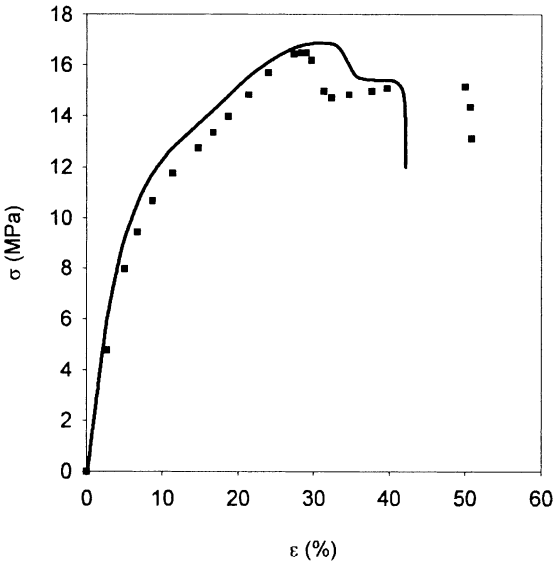

Fig. 6. Tensile curves at 120°C of IM samples as-delivered (square) and standardised (full line); displacement rate = 0.01 cm/min.

When measuring at 23 and 40°C, effects are sometimes similar but more defined at 23°C (Fig. 8). Thus E_N is always lower and E_{23} and E_{40} higher. But deformability is lower after annealing at 23 and 40°C, as deformation at 30 MPa stress is lower (Table 1). Also the yield stress increases after these treatments as compared to standardisation. This is especially observed for CM.

We notice the same evolution during the creep tests for the compliance in the linear range (Fig. 5). The compliance is higher after standardisation annealing and lower after annealing at 40°C, but they all converge in the field of high deformation (non-linear).

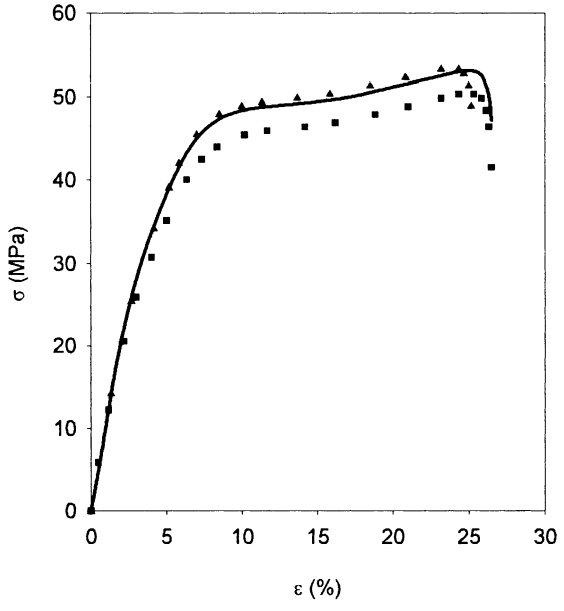

Fig. 7. Tensile curves at 23°C of IM samples annealed 1 day (square), 10 days (full line) at 23°C and 1 day at 40°C (triangle); displacement rate = 0.01 cm/min.

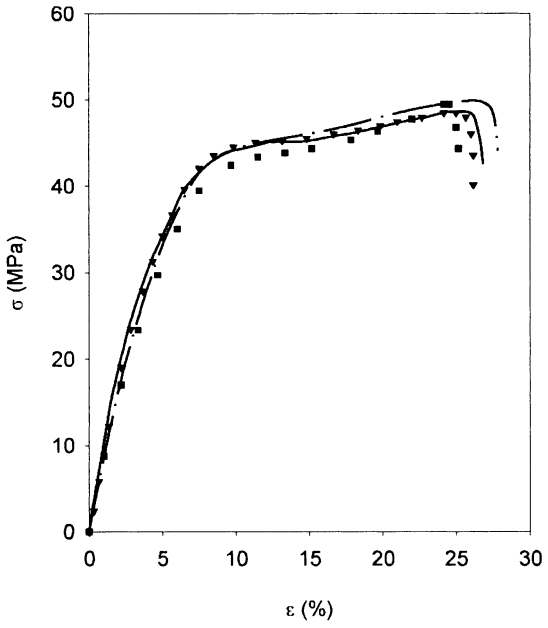

Fig. 8. Tensile curves at 23°C of IM samples standardised (square), annealed 10 days at 23 (full line), 40 (triangle) and at 80°C (dash-dot); displacement rate = 0.01 cm/min.

For drawing at 120°C (Table 5), the observed effects are different for CM. Thus, E_{80} and E_N are higher than E_{23} and E_{40} and deformability decreases after standardisation or annealing at 80°C.

4. Discussion

4.1. Processing

Injection moulding requires the control of more parameters than for compression moulding [13]. We can analyse effects of those two techniques on processed material along two scales:

1. on a small scale, IM are more homogeneous owing to a stricter control of temperature, as well as orientation due to applied shear in the screw and during injection into the cold mould. This implies more perfect and more oriented crystals in IM compared to CM, which undergo neither shear nor quench.
2. on a large scale, IM are more heterogeneous [14] due to temperature heterogeneity across the sample thickness. Thus the surface, in contact with the mould, cools more quickly than the sample core, so the crystalline size varies according to its position across the thickness. The CM samples are cooled to room temperature, without contacting any cold surface, so temperature is more homogeneous across the thickness compared to IM.

Also, the cooling rate is higher for IM than CM. This

influences considerably the crystalline size. We have then a much larger number of small crystals in IM, compared to CM.

This implies also, a larger a–c interface region content in IM than in CM for an equal crystalline phase quantity. But in the previous work [12], thermal and dynamic measurements have demonstrated that there is more amorphous and less crystalline phase in IM with respect to CM; this has been explained due to incomplete crystallisation in IM as a consequence of quenching in the mould. This additionally explains the lower storage modulus for IM in all temperature ranges compared to CM. This is also shown for Young's modulus (Tables 1–5), which is higher for CM in almost all cases.

The necking that appears in CM after yield is due to the presence of more defects, and an easy localisation of deformation, although the crystals are larger than in IM. However in the latter case, they are more homogeneous and more oriented, leading to more strain hardening, making strain localisation more difficult. This eases reorganisation in TTT (β) conformation from GTGT (α), or from the a–c interfacial region or even from the amorphous phase [12].

Concerning IMB samples, the β conformation is already present, so little or no reorganisation takes place during drawing, favouring deformation localisation and the appearance of necking.

During drawing at 120°C, the material becomes more fragile and chain mobility increases, even inside the crystallites since they are able to crystallise at this temperature. This induces necking even in IM, although less so than in CM.

4.2. Standardisation annealing

This annealing effectively normalises all samples produced by the same processing technique. A major part of the thermomechanical history is recorded in the crystalline phase formed during processing at temperatures above 150°C, so IM and CM behaviour remains different even after standardisation.

The increase of storage modulus after this annealing, compared with the as-delivered samples, for IM in low and high temperature ranges is mainly due to the increase of crystallinity [12] which reinforces the material in this temperature area. At low temperature, all phases have a high modulus but the crystalline phase has the highest, resulting in the increase of sample modulus with crystallinity. At high temperatures, the amorphous and a–c interfacial region are in equilibrium and therefore very mobile and soft, only the crystalline phase remains compact and rigid so that the modulus also increases with crystallinity. We observe the same evolution during drawing at 120°C for CM (Table 5); we have thus an increase of Young's modulus after standardisation annealing compared with the as-delivered samples.

At room temperature, only the amorphous phase is soft. The a–c interfacial region becomes rigid and its increase induces a higher modulus whereas its absence decreases the storage and Young's modulus. This occurs after standardisation annealing, when the interfacial region fraction decreases or even disappears leading to a decrease of Young's modulus for all samples. This implies also an increase of compliance at short times, and its decrease at long times due to the increase in crystallinity.

4.3. Post-standardisation annealing

The effects of these treatments are particularly evident during tests at 23°C. At this temperature, the effects of annealing during the tests are the weakest, compared to those during tests at 40 or 120°C, where changes operate more rapidly.

When annealing at 23 and 40°C, the a–c interfacial region forms at the expense of the amorphous phase [12]. The a–c interfacial region quantity is higher after annealing at 23°C, but more stable after that at 40°C, thus its transition temperature is higher. Therefore the modulus is higher during drawing at 23°C after annealing at 40°C, and the compliance is lower. During annealing at 80°C, a–c interfacial region does not form because this temperature is above Tg_U and it does not have enough time to form when cooling to 23°C. Thus this annealing does not differ much from standardisation.

During drawing at 40°C, the effects of annealing at 23°C are partly deleted. Thus E_{23} is lower than E_{40}.

When drawing at 120°C, the crystalline phase dominates the behaviour. DSC results on CM showed that crystalline quantity is influenced by cooling rate [12]. Thus we have a higher quantity when annealing at 80°C or standardisation than at 23 or 40°C, and therefore a higher Young's modulus after the first two treatments.

5. Conclusions

This work has demonstrated the influence of structure on the mechanical behaviour of PVDF. Major differences are observed when using different processing techniques. These differences remain in spite of final annealing at temperatures below the melting temperature of PVDF. Differences appear mainly after yield in tensile drawing, because of the formation of the β conformation for IM and not for CM, and the participation of the crystalline phase in the materials behaviour depending on measurement temperature.

Concerning the nature of these variations and their kinetics, they evolve differently depending on the temperature position with respect to Tg_U. Mechanical characteristics depend thus on annealing and measurement temperatures.

Although differences due to processing cannot be erased by the thermal treatments investigated in this work, an improvement, particularly in long-term mechanical

behaviour, can be obtained by the use of an appropriate annealing treatment.

Acknowledgements

The authors wish to thank Solvay S.A. for providing the materials used in this investigation. One of us (B.-E. El Mohajir) is grateful for financial support from 'Fondation Universitaire David et Alice Van Buuren' in the course of this work.

References

[1] Rault J. Semi-crystalline polymers; influence of the molecular weight on the morphology and the mechanical properties. In: Escaig B, G'sell C, editors. Plastic deformation of amorphous and semi-crystalline materials. Les editions de Physique, 1982. p. 313–25.
[2] Ludwig BW, Urban MW. Polymer 1997;38(9):2077–91.
[3] Peterlin A. Colloid and Polymer Sci 1987;265:357–82.
[4] Flory PJ, Yoon DY. Nature 1978;272:226–9.
[5] Haudin JM. Plastic deformation of semi-crystalline polymers. In: Escaig B, G'sell C, editors. Plastic deformation of amorphous and semi-crystalline materials. Les editions de Physique, 1982. p. 291–311.
[6] Haudin JM, G'Sell C. Mécanismes microscopiques de déformation des polymères semi-cristallins. In: G'sell C, Haudin JM, editors. Introduction à la mécanique des polymères. INPL, 1995. p. 251–73.
[7] Gent AN, Madan SJ. Polym Sci: Part B: Polym Phy 1989;27:1529–42.
[8] Takahashi Y, Zakoh T, Hanatani N. Colloid Polym. Sci. 1991;269:781–4.
[9] Kalfoglou NK, Williams H, Leverne. J Appl Polym Sci 1973;17:3367–73.
[10] Teyssedre G, Grimau M, Bernes A, Martinez JJ, Lacabanne C. Polymer 1994;35(20):4397–403.
[11] Teyssedre G, Bernes A, Lacabanne CJ. Polym Sci: Part B: Polym Phy 1993;31:2027–34.
[12] El Mohajir B-E., Heymans N. Polymer 2001;42(13):5661–7.
[13] Glanvill AB. Injection moulding. In: Ogorkiewicz RM, editor. Thermoplastic effects of processing. London: Iliffe Books Ltd for The Plastics Institute, 1969. p. 110–82.
[14] Wang YD, Cakmak MJ. Appl Polym Sci 1998;68:909–26.